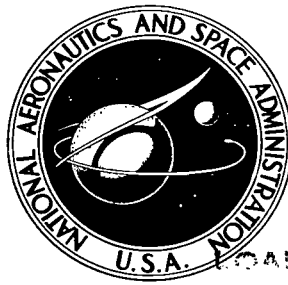


NASA TECHNICAL NOTE

NASA TN D-8403



NASA TN D-8403 c.1

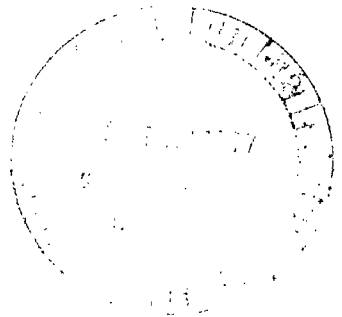
LOAN COPY: RE
AFWL TECHNICAL
KIRTLAND AFB



**WELDABILITY OF HIGH-TOUGHNESS IRON -
12-PERCENT-NICKEL ALLOYS WITH
REACTIVE METAL ADDITIONS OF
TITANIUM, ALUMINUM, OR NIOBIUM**

*Jack H. Devletian, Joseph R. Stephens,
and Walter R. Witzke*

*Lewis Research Center
Cleveland, Ohio 44135*





0134122

1. Report No. NASA TN D-8403		2. Government Accession No.		3. Recipient's Catalog No.	
4. Title and Subtitle WELDABILITY OF HIGH-TOUGHNESS IRON - 12-PERCENT-NICKEL ALLOYS WITH REACTIVE METAL ADDITIONS OF TITANIUM, ALUMINUM, OR NIOBIUM				5. Report Date February 1977	
				6. Performing Organization Code	
7. Author(s) Jack H. Devletian, Joseph R. Stephens, and Walter R. Witzke				8. Performing Organization Report No. E-8883	
				10. Work Unit No. 506-16	
9. Performing Organization Name and Address Lewis Research Center National Aeronautics and Space Administration Cleveland, Ohio 44135				11. Contract or Grant No.	
				13. Type of Report and Period Covered Technical Note	
12. Sponsoring Agency Name and Address National Aeronautics and Space Administration Washington, D.C. 20546				14. Sponsoring Agency Code	
15. Supplementary Notes					
16. Abstract Three exceptionally high-toughness Fe-12Ni alloys designed for cryogenic service were welded by using the gas-tungsten arc (GTA) welding process. Evaluation of their weldability included equivalent-energy fracture toughness K_{Icd} tests, transverse-weld tensile tests at -196° and 25° C, and weld crack sensitivity tests. The Fe-12Ni-0.25Ti alloy proved extremely weldable for cryogenic applications, having weld and heat-affected zone (HAZ) properties comparable to those of the wrought base alloy. The Fe-12Ni-0.5Al alloy had good weld properties only after the weld joint was heat treated. The Fe-12Ni-0.25Nb alloy was not considered weldable for cryogenic use because of its poor weld-joint properties at -196° C and its susceptibility to hot cracking.					
17. Key Words (Suggested by Author(s)) Weldability; Gas tungsten arc weld; Iron-nickel alloys; Reactive metal additions; Fracture toughness; Cryogenic; Liquid nitrogen; Yield strength; Titanium; Aluminum; Niobium				18. Distribution Statement Unclassified - unlimited STAR Category 26	
19. Security Classif. (of this report) Unclassified		20. Security Classif. (of this page) Unclassified		21. No. of Pages 22	
				22. Price* A02	

CONTENTS

	Page
SUMMARY	1
INTRODUCTION	2
EXPERIMENTAL PROCEDURE	2
Materials	2
Procedure	3
Welding	3
Fracture toughness test	4
Tensile tests	4
Weld cracking test	5
Electron microprobe	5
Metallography	5
RESULTS	5
Fracture Toughness	5
Tensile Properties	6
Crack Susceptibility of Welds	7
Chemistry - Metal Transfer Through Arc	7
Weld Microstructure	8
Electron-Microprobe Analyses	8
DISCUSSION	9
Fracture Toughness	9
Weld Cracking and Tensile Properties	10
Applicability of Other Welding Processes	10
CONCLUDING REMARKS	11
CONCLUSIONS	11
REFERENCES	12

WELDABILITY OF HIGH-TOUGHNESS IRON - 12-PERCENT-NICKEL ALLOYS WITH REACTIVE METAL ADDITIONS OF TITANIUM, ALUMINUM, OR NIOBIUM

by Jack H. Devletian,* Joseph R. Stephens, and Walter R. Witzke

Lewis Research Center

SUMMARY

The weldabilities of three high-strength, high-toughness Fe-12Ni alloys were investigated. These experimental alloys were Fe-12Ni-0.25Ti, Fe-12Ni-0.5Al, and Fe-12Ni-0.25Nb. Gas-tungsten arc (GTA) welds were deposited on 0.1- and 0.7-cm-thick workpieces using filler metal of the same composition as that of the base alloy. Equivalent-energy fracture toughness K_{Icd} and transverse-weld tensile behavior were evaluated at 25° and -196° C. Additional evaluation included weld-crack susceptibility tests, electron microprobe analyses, metallography, and X-ray diffraction.

At -196° C the Fe-12Ni-0.25Ti alloy possessed excellent as-welded fracture toughness in the weld and the heat-affected zone (HAZ). In addition, the weld and HAZ toughnesses were not significantly influenced by the weld cooling rate, implying that virtually any thickness of this alloy could be welded. The toughnesses of the Fe-12Ni-0.5Al alloy weld and HAZ were low at -196° C but were effectively increased to the level of the base alloy by postweld quench annealing at 550° C. The Fe-12Ni-0.25Nb alloy weld had the poorest fracture toughness in the as-welded condition, only 14 percent of the base alloy toughness.

The transverse-weld tensile properties at 25° and -196° C of the titanium- and aluminum-bearing alloys were comparable to those of the wrought base alloy since these tensile specimens always failed in the base alloy. However, the transverse-weld tensile properties of the niobium-bearing alloy at -196° C were erratic.

Circular patch tests of weld-crack susceptibility showed that welds deposited on the aluminum- and titanium-bearing alloys were resistant to weld cracking but that welds deposited on the niobium-bearing alloy tended to hot crack readily.

Based on these evaluations, the Fe-12Ni-0.25Ti alloy is considered a fully weldable cryogenic material that requires neither pre- nor postweld heat treatment to be welded in virtually any thickness. The Fe-12Ni-0.5Al alloy also has excellent weldability provided each weld joint is postweld quench annealed at 550° C. The Fe-12Ni-0.25Nb alloy is not considered weldable.

*Assistant Professor of Materials Science, Youngstown State University, Youngstown, Ohio; Summer Faculty Fellow at the Lewis Research Center in 1975 and 1976.

INTRODUCTION

The need for alloys in cryogenic service has increased substantially during recent years. For example, the transport and storage of liquefied natural gas (which boils at -160°C) requires large amounts of alloys for cryogenic service. Iron-base alloys that are currently in use or that are being considered for cryogenic applications include 304 stainless steel, 9 nickel steel, and 5 nickel steel (ref. 1). The 304 stainless steel is a high-toughness - low-strength alloy, but the 9 and 5 nickel steels have somewhat lower toughness at higher strength levels.

In an alloy development study at the University of California (ref. 2), an experimental Fe-12Ni-0.3Ti alloy that had been heat treated to produce an extremely fine grain size exhibited the same toughness at -196°C as 304 stainless steel and was as strong as the 9 nickel steel. More recently, Witzke and Stephens (ref. 3) have identified several reactive metal additions that improve the -196°C toughness of the Fe-12Ni alloy without the need for complex grain-refining heat treatments. For these experimental alloys to be usable at cryogenic temperatures, their ability to be welded without sacrificing a substantial degree of toughness and strength must be demonstrated.

This investigation was made to determine the relative weldability of the three most promising experimental Fe-12Ni-reactive metal alloys identified in reference 3. The three alloys selected were Fe-12Ni-0.25Ti, Fe-12Ni-0.5Al, and Fe-12Ni-0.25Nb.¹ These alloys all have excellent tensile strength and fracture toughness at cryogenic temperatures. Welding by the inert gas-tungsten arc (GTA) technique was performed on 0.1-cm-thick sheet and on 0.7-cm-thick plate. Equivalent-energy fracture toughness K_{Icd} testing was the primary means of assessing the weldability of these experimental alloys. In addition, transverse-weld tensile tests, circular patch tests, and supplementary metallographic and electron microprobe evaluations were conducted.

EXPERIMENTAL PROCEDURE

Materials

The Fe-12Ni alloys used in this investigation were prepared from vacuum-processed iron rod of 99.95-wt % purity, electrolytic nickel chips containing less than 100-ppm (by weight) total interstitial impurities, and the reactive metals titanium (containing less than 5000-ppm interstitial impurities) and aluminum and niobium (with less than 100-ppm total O, N, and C).

¹ All experimental alloy compositions in this report are given in atomic percent.

Ingots were prepared by nonconsumable arc melting of 1000-gram charges in a 7.5-cm by 7.5-cm by 3-cm-deep water-cooled copper mold after evacuating and backfilling with argon to one-half atmospheric pressure. To adequately homogenize the ingots, each was given a minimum of four melts.

Two ingots of each alloy were hot rolled at 1100°C after annealing for $1/2$ hour at that temperature. The rolling procedure included 15-percent reductions per pass and two rolling passes per 5-minute reheat. For each alloy, the first ingot was rolled to a thickness of 0.1 cm and the second was rolled to a thickness of 0.7 cm. These two sizes were selected because the 0.1-cm thickness is used in fabricating commercial cryogenic containers and the 0.7-cm thickness was required for fracture toughness evaluation.

The 0.1-cm-thick, hot-rolled sheet was prepared for welding by shearing it into 8.9-cm by 7.6-cm sections. The 0.7-cm-thick, hot-rolled plate was machined into 6.4-cm by 5.1-cm sections each containing a double-V groove, as shown in figure 1(a). Approximately two-thirds of the sections were heat treated to achieve maximum fracture toughness at -196°C prior to welding. This heat treatment varied for each alloy (ref. 3): The Fe-12Ni-0.25Ti alloy was annealed for 2 hours at 685°C in an argon atmosphere, followed by a rapid brine quench. The Fe-12Ni-0.5Al and Fe-12Ni-0.25Nb alloys were similarly quench annealed at 550°C and 820°C , respectively. All specimens to be welded were grit blasted and cleaned in acetone. Some of the welded specimens were postweld quench annealed by the procedures described.

Procedure

Welding. - Full-penetrating, single-pass welds were deposited on all 0.1-cm-thick sheet specimens by using the autogenous GTA welding process with $200\text{-cm}^3/\text{sec}$ argon gas shielding. All 0.7-cm-thick specimens were GTA welded in four passes (pass sequence shown in fig. 1(b)) by using 0.23-cm-diameter filler metal swaged from the base metal. Welding parameters were 50 to 100 A, 9 to 11 V, and 15- to 25-cm/min travel speed for the 0.1-cm-thick sheet and 130 to 140 A, 11 to 13 V, and 10- to 15-cm/min travel speed for the 0.7-cm-thick specimens.

Weld cooling rates were measured at 700°C for each weld by plunging a 0.038-cm-diameter W/W-26Re thermocouple directly into the weld pool. Cooling curves for each weld were recorded on a continuous chart recorder. Three weld cooling rates, from 3° to 142°C per second, were investigated. Slow weld cooling rates were obtained by preheating the workpiece to 260°C . Extremely fast cooling rates were obtained by tightly clamping a 0.7-cm-thick copper backup plate to the workpiece. Intermediate or normal weld cooling rates were obtained by allowing the weld metal to cool in air with neither preheating nor backup material.

Fracture toughness test. - Slow-bend test specimens were used to determine the fracture toughness of both the weld and the heat-affected zone (HAZ). The test specimens were 5.08-cm by 1.00-cm by 0.64-cm notched Charpy bars. Two sets of bars without notches were first machined from the welded sections. Each bar was etched with 2 percent Nital to reveal the weld location so that the notch on one set could be machined in the weld metal and the notch in the second set could be machined in the HAZ. Each specimen was then fatigue cracked to an initial ratio of crack length to specimen width a/W of approximately 0.4. Testing was conducted in a three-point bending apparatus immersed in a liquid-nitrogen bath or at room temperature. The specimens were positioned between a 0.64-cm-diameter center roller and two similar support rollers to provide a support span of 3.81 cm. A crosshead speed of 0.13 cm/min was used. A load/displacement curve was generated from the outputs of a load cell that supported the bend apparatus and a double-cantilevered clip-on displacement gage (ref. 4). This gage sensed the crack opening displacement through the vertical movement of a ceramic rod riding on the bend bar. The fracture toughness parameter K_{Icd} was determined from load/displacement curves by using the K_{Ic} equation for a slow-bend test specimen given in ASTM standard E399 (ref. 4) as modified by the empirical equivalent energy method (ref. 5). The relation used for calculating the fracture toughness of a slow-bend test specimen was

$$K_{Icd} = \frac{SP_2 \sqrt{\frac{A_1}{A_2}} f\left(\frac{a}{W}\right)}{BW^{3/2}}$$

where

S span

P_2 any load on linear portion of load/displacement curve

A_1 area under curve to maximum load

A_2 area under curve to P_2

a specimen crack depth

W specimen width

$f(a/W)$ value of power series for a/W (given in ref. 4)

B specimen thickness

The fracture toughness data presented are generally values obtained from single tests.

Tensile tests. - Flat transverse-weld tensile specimens with reduced section dimensions of 0.10 cm by 0.63 cm and a gage length of 2.54 cm were tested at 25° and

-196° C at a crosshead speed of 0.13 cm/min. Similar unwelded specimens also were tested to provide reference base alloy properties.

Weld cracking test. - The standard circular patch test for crack susceptibility (test 61 in ref. 6) was employed to determine the resistance of each alloy to hot and cold weld cracking. Gas-tungsten arc welds were deposited along a 5.1-cm-diameter circle on 0.1-cm-thick sheets. Welding was done manually at room temperature.

Electron microprobe. - Microprobe analyses, using the specimen traverse technique, were conducted on the weld metal and the HAZ to detect the presence and distribution of nickel, titanium, aluminum, and niobium in the Fe-12Ni alloys.

Metallography. - All welded joints were sectioned transversely for metallographic examination. Etchants employed included standard 2-percent Nital to reveal the cellular solidification structure; and a three-acid etchant consisting of 1 part by volume hydrofluoric acid, 33 parts nitric acid, and 33 parts acetic acid in 933 parts water to show the weld structure resulting from solid-state transformations.

RESULTS

The weldabilities of Fe-12Ni alloys containing additions of titanium, niobium, and aluminum were evaluated by equivalent-energy fracture toughness K_{Icd} and transverse-weld tensile tests. Results from these tests are presented in tables I and II, respectively. Unless otherwise indicated, all weld properties cited herein are for welds made under intermediate or normal cooling rates.

Fracture Toughness

At -196° C, the Fe-12Ni-0.25Ti alloy had high as-welded K_{Icd} fracture toughness values (227 to 347 MPa \sqrt{m}) in both the weld and the HAZ with or without preweld heat treatment. These toughness levels compared favorably with that of the base alloy (275 MPa \sqrt{m}) that had been quench annealed at 685° C for maximum toughness as shown in figure 2. Postweld heat treating had little effect on the toughness of the weld or the HAZ of this alloy. As shown in figure 3(a), minor increases in weld and HAZ fracture toughness values were observed as the weld cooling rate was increased.

For the Fe-12Ni-0.5Al alloy at -196° C, the weld and HAZ fracture toughness values in the as-welded condition (with or without preweld heat treatment) were generally poor: 69 to 81 MPa \sqrt{m} as compared with 284 MPa \sqrt{m} for the heat-treated base alloy, as shown in figure 2. However, postweld quench annealing these welded specimens at 550° C effectively increased the weld and HAZ toughness values (275 and 300 MPa \sqrt{m} ,

respectively) to approximately the level of the base alloy. From figure 3(b), the weld cooling rate had no significant effect on the weld or HAZ toughness values for this alloy.

The as-welded fracture toughness values of the Fe-12Ni-0.25Nb alloy at -196°C were also poor: 47 to 205 $\text{MPa}\sqrt{\text{m}}$ as compared with 329 $\text{MPa}\sqrt{\text{m}}$ for the quench-annealed base alloy (fig. 2). With postweld quench annealing at 820°C , the HAZ toughness value (320 $\text{MPa}\sqrt{\text{m}}$) was effectively raised to the level of the base alloy, but the toughness of the weld (213 $\text{MPa}\sqrt{\text{m}}$) remained significantly below that of the base alloy (329 $\text{MPa}\sqrt{\text{m}}$). As shown in figure 3(c), the weld cooling rate had only a minor effect on toughness.

Fracture toughness trends observed at 25°C were similar to those at -196°C , as shown in figure 4. The titanium-containing alloy had relatively high weld and HAZ fracture toughness values: 188 and 264 $\text{MPa}\sqrt{\text{m}}$, respectively, in the as-welded condition as compared with 276 $\text{MPa}\sqrt{\text{m}}$ for the quench-annealed base alloy. The corresponding weld toughness values for the aluminum- and niobium-bearing alloys at 25°C were significantly lower than their respective base-alloy toughness levels.

Tensile Properties

The transverse-weld tensile properties at -196°C of the Fe-12Ni-0.25Ti alloy (fig. 5) compared closely with those of the quench-annealed base alloy. The weld cooling rate did not affect its tensile properties, and all transverse-weld specimens failed outside the weld. Postweld quench annealing of these specimens resulted in no major changes in tensile properties, as shown in figure 6.

At -196°C , the weld-joint tensile properties of the Fe-12Ni-0.5Al alloy (fig. 5) were comparable to those of the base alloy except for tensile elongation. The weld-joint elongation of 12 percent was far below the 28 percent recorded for the base alloy in the quench-annealed condition. All fractures of the transverse-weld tensile specimens occurred outside both the weld and the HAZ. The weld cooling rate had no appreciable effect upon tensile properties, as shown in figure 5. Postweld quench annealing at 550°C resulted in a minor increase in elongation accompanied by corresponding decreases in tensile and yield strengths (fig. 6).

The weld-joint tensile properties of Fe-12Ni-0.25Nb at -196°C were comparable to those of the quench-annealed base alloy only when the transverse-weld specimen failed outside the weld (fig. 5). Tensile failures occurring within the weld zone resulted in lower and more erratic tensile properties. For example, the elongation and yield strength values of transverse-weld specimens failing outside the weld had elongations of 10 to 11 percent and yield strengths of 958 to 979 MPa; those specimens failing in the weld had elongations of 0 to 6 percent and yield strengths of 820 to 965 MPa. The weld cooling rate appeared to have little effect upon weld-joint properties. As shown in

figure 6, postweld quench annealing at 820° C tended to improve ductility and to decrease the occurrence of weld metal failures.

The weld-joint tensile properties at 25° C of the Fe-12Ni alloys containing titanium, aluminum, and niobium (fig. 7) displayed the following general similarities: (1) all transverse-weld tensile specimens failed outside the weld, (2) the weld cooling rate had virtually no effect on tensile properties, (3) the weld-joint properties for each alloy tended to parallel those of the quench-annealed base alloy, and (4) postweld quench annealing resulted in very little change in elongation and only slight decreases in tensile and yield strengths (table II).

Crack Susceptibility of Welds

Gas-tungsten arc welds made on 0.1- and 0.7-cm-thick specimens of Fe-12Ni-0.25 Ti and Fe-12Ni-0.5Al alloys were defect free as evidenced by radiographic inspection. However, cracking problems were encountered when the 0.7-cm-thick specimens of Fe-12Ni-0.25Nb alloy were GTA welded by using filler metal of the same composition as the base alloy. This alloy exhibited strong hot-cracking tendencies during the first and second passes of the four-pass weld (welding sequence shown in fig. 1(b)). No cracking resulted when the relatively unrestrained 0.1-cm-thick sheet specimens were GTA welded.

Standard circular patch tests (ref. 6), using the 5.1-cm-diameter GTA weld circle, verified these hot-cracking observations. The aluminum- and titanium-bearing alloys had excellent resistance to hot and cold cracking, while the niobium-bearing alloy showed extensive hot cracking along the centerlines of each weld.

Chemistry - Metal Transfer Through Arc

High transfer efficiencies (i. e. , transfer of alloying elements from filler metal to weld) were obtained in this investigation for the major alloying elements nickel, titanium, aluminum, and niobium during GTA welding (table III). Even titanium, which is one of the most difficult elements to transfer across a welding arc, was successfully transferred with an efficiency of 81 percent.

The GTA welding process effectively protected the molten weld pool from interstitial contamination from the atmosphere. Comparing the oxygen, nitrogen, and carbon contents of the weld metal and the adjacent base alloy (table III) showed that the interstitial content was low in both regions.

Weld Microstructure

The solidification structures of all three Fe-12Ni alloys (as revealed by etching in Nital) were typically cellular over the wide range of weld cooling rates investigated (3° to 142° C per sec). Each weld metal grain grows epitaxially from the HAZ and contains the cellular substructure (fig. 8(a)). Postweld quench annealing to maximize toughness had little effect on the solidification structure (fig. 8(b)).

These welds were repolished and etched with the three-acid etchant to reveal the weld microstructures associated with solid-state transformations during weld cooling. Results showed only minimal effects from additions of titanium, aluminum, and niobium to the Fe-12Ni base alloy. Figures 9(a-1), (b-1), and (c-1) show the weld microstructures of titanium-, aluminum-, and niobium-bearing alloys in the as-welded condition to be essentially all martensitic. Our X-ray diffraction studies of these alloy welds clearly indicated the presence of at least 99-percent martensite, with the remaining 1 percent attributed to retained austenite. The wide range of weld cooling rates used in this investigation had no significant effect on the resulting martensitic structure. The only characteristic microstructural feature resulting from the addition of titanium, aluminum, and niobium was the precipitation of interstitial compounds, which appear as widely scattered microscopic particles in figure 9.

The metallurgical condition of the workpiece prior to welding had no appreciable effect on the weld microstructure. Welds deposited on both hot-rolled sheet and quench-annealed sheet had essentially identical weld and HAZ microstructures, similar to those shown in figures 8 and 9, for all three alloys tested.

Postweld heat treating of the martensitic weld structures to attain maximum fracture toughness had several significant effects on the microstructures. The Fe-12Ni-0.25Ti alloy weld was quench annealed at 685° C, which is in the ferrite-plus-austenite range. This weld microstructure (fig. 9(a-2)) contains a fine, laminated morphology of ferrite (light) and tempered martensite (dark). Quench annealing the Fe-12Ni-0.5Al alloy weld at 550° C effectively tempered the as-welded martensitic structure, as shown in figure 9(b-2). Quench annealing the Fe-12Ni-0.25Nb alloy weld at 820° C produced a fine-grained martensitic structure, shown in figure 9(c-2).

Electron-Microprobe Analyses

Results from microprobe scans across the welds of the three experimental alloys indicated that nickel segregated strongly at practically all solidification cell boundaries. For example, with the Fe-12Ni-0.25Nb alloy, nickel peaks occurred at every optically observed cell boundary (fig. 10 shows a segment of the nickel and niobium scans). About three-fourths of the strong niobium peaks occurred at these same boundary locations.

The sole noncorresponding niobium peak in this figure, indicated by the letter "A," occurred at a niobium-rich precipitate within a cell. In the weld metal of the aluminum- and titanium-bearing alloys, somewhat weaker aluminum and titanium peaks were detected at cell boundaries. Since the detection limit of these elements in the scanning mode was about 0.1 percent by weight, small concentration gradients of titanium, aluminum, and niobium between cell centers and peripheries could not be detected. No significant segregation of alloying elements was observed in the HAZ.

DISCUSSION

Fracture Toughness

The most promising alloy from a weldability viewpoint is the Fe-12Ni-0.25Ti alloy. This alloy exhibited the highest weld and HAZ equivalent-energy fracture toughness K_{Icd} values at 25° and -196° C in the as-welded condition. From figures 2 to 4, the weld and HAZ fracture toughness values of this alloy were about equivalent to those of the base alloy, which was quench annealed at 685° C for maximum toughness. However, even more important is the fact that the HAZ toughness value in the as-welded condition actually exceeded that of the base alloy. This is extremely significant from a structural point of view because the HAZ is an inherent part of the wrought base alloy. The toughness of the HAZ cannot be changed except by postweld heat treatment, which may, in many cases, be impractical or uneconomical. On the other hand, virtually any value of toughness may be obtained in the weld metal by simply choosing the appropriate filler metal composition. Thus, a high-toughness alloy that has a high HAZ toughness in the as-welded condition is ideal for welding applications in the field, where postweld heat treating is unfeasible. This points up a potential commercial advantage of the Fe-12Ni-0.25Ti alloy over the niobium- and aluminum-bearing alloys, which have poor as-welded toughness in the HAZ. Furthermore, the weld and HAZ toughness of the titanium-bearing alloy was unaffected by the weld cooling rate (figs. 3 and 4). As a result, welds could be made on practically any thickness of sheet or plate while still maintaining high toughness. Finally, the cost of filler metal is substantially reduced without an appreciable loss in overall weld-joint toughness by using the Fe-12Ni-0.25Ti alloy filler metal to replace the more expensive nickel-base fillers that are commonly used to weld Fe-9Ni alloys (ref. 7).

For applications where the welds can be postweld heat treated to maximum toughness, the aluminum-bearing alloy also becomes attractive. Although the weld and HAZ toughness values at -196° C of the Fe-12Ni-0.5Al alloy (fig. 2) were poor in the as-welded condition, they were excellent after quench annealing at 550° C, equaling that of the base metal. Therefore, all cryogenic structural applications using the aluminum-bearing alloy would require postweld quench anneal.

The most difficult weldability problems were encountered with the Fe-12Ni-0.25Nb alloy, which had the highest wrought alloy toughness of the three alloys investigated. Welds made from this alloy were not only hot-crack sensitive and low in toughness but also inadequately responsive to postweld quench annealing (fig. 2). Clearly, welding the niobium-bearing alloy would require development of a tough filler alloy for higher weld-metal toughness.

Weld Cracking and Tensile Properties

The titanium- and aluminum-bearing alloys have good resistance to weld cracking, but the niobium-bearing alloy is plagued with a serious hot-cracking problem. Unless a suitable filler metal is developed, the general usefulness of the Fe-12Ni-0.25Nb alloy as a fabricable cryogenic steel would be severely limited.

Except for lower ductility in the aluminum-bearing alloy welds, the transverse-weld tensile properties at -196°C of the titanium- and aluminum-bearing alloys were generally comparable to their respective quench-annealed base alloy properties since all failures occurred in the base alloy. Only the niobium-bearing alloy displayed erratic transverse-weld tensile properties (fig. 5). The scope of this work does not permit a full explanation of this behavior at -196°C . However, the low solubility of niobium in iron (<0.5 at. %) as compared with solubilities of approximately 8 and more than 20 at. % for titanium and aluminum, respectively, in iron may partially account for the erratic behavior of the niobium-bearing alloy. Cell boundary segregation of reactive metals in the weld was more prominent in the niobium-bearing alloy, as evidenced by electron microprobe results. This suggests that the lower solubility of niobium in iron led to this high level of segregation, which may be a cause of the poor weld properties of this alloy.

The transverse-weld tensile properties at room temperature of the three alloys studied were all generally comparable to those of their respective base alloys. Since all failures occurred outside the weld, design parameters for welded joints in room-temperature applications could be based on the lower base-alloy strength properties rather than on those of the weld.

Applicability of Other Welding Processes

In this investigation, the GTA welding process was used because it is the "cleanest," commonly used process for welding sheet. The dense argon gas adequately shields the molten Fe-12Ni alloy welds from interstitial contamination (table III). Although only the GTA welding process was studied herein, we can speculate about the applicability of other welding processes. Other welding processes that similarly protect the molten weld

pool from the atmosphere should also be suitable; for example, gas-metal arc, plasma arc, resistance, diffusion, or electron-beam welding. However, potentially contaminating processes such as shielded-metal arc, submerged arc, flux-cored gas-metal arc, or electroslag welding probably are not applicable for these alloys since contamination could lead to low fracture toughness. Furthermore, the shielding gas required to weld Fe-12Ni alloys must be dry and inert (such as dry argon or helium) and not reactive like carbon dioxide or oxygen.

CONCLUDING REMARKS

The strikingly high weld and HAZ toughness combined with good transverse-weld tensile properties emphasizes the great potential of the Fe-12Ni-0.25Ti alloy as a fully weldable and fabricable cryogenic alloy. Neither pre- nor postweld heat treatments are required to GTA weld virtually any thickness of this alloy. Yet, the average weld and HAZ toughness levels are approximately equal to those of the quench-annealed base alloy. However, to weld this alloy properly and to efficiently transfer titanium across the welding arc, it is necessary to use a welding process that fully protects the molten weld pool from interstitial contamination. The widely used GTA welding technique is such a process.

CONCLUSIONS

The effects of gas-tungsten arc (GTA) welding on Fe-12Ni alloys containing small additions of titanium, aluminum, or niobium were evaluated by equivalent-energy fracture toughness K_{Icd} and tensile studies of welded specimens at -196° and 25° C. Based on this study, the following conclusions were reached:

1. The Fe-12Ni-0.25Ti alloy is weldable in virtually any thickness without pre- or postweld heat treatment and can achieve weld properties comparable to those of the base alloy.
2. The Fe-12Ni-0.5Al has good weldability but develops original toughness and strength only after a postweld heat treatment.
3. The Fe-12Ni-0.25Nb alloy is not weldable because of severe hot-cracking tendencies and poor mechanical properties in the weld and the heat-affected zone.
4. The GTA welding process is an excellent method for welding Fe-12Ni alloys.

Lewis Research Center,
National Aeronautics and Space Administration,
Cleveland, Ohio, November 2, 1976,
506-16.

REFERENCES

1. Kaufman, J. G.: Symposium on Properties of Materials for Liquefied Natural Gas Tankage. Am. Soc. Test. Mater. STP 579, 1975.
2. Jin, Sungho; Hwang, S. K.; and Morris, J. W., Jr.: Comparative Fracture Toughness of an Ultrafine Grained Fe-Ni Alloy at Liquid-Helium Temperature. Metall. Trans. A, vol. 6A, no. 8, Aug. 1975, pp. 1569-1575.
3. Witzke, Walter R.; and Stephens, Joseph R.: Effect of Minor Reactive Metal Additions on Fracture Toughness of Iron - 12-Percent-Nickel Alloy at -196° and 25° C. NASA TN D-8232, 1976.
4. Plane-Strain Fracture Toughness of Metallic Materials. Am. Soc. Test. Mater. Stand. E-399-74, 1974.
5. Witt, F. J.; and Mager, T. R.: Procedure for Determining Bounding Values on Fracture Toughness K_{Ic} at Any Temperature. ORNL-TM-3894, Oak Ridge National Lab., 1972.
6. Randall, M. D.; Monroe, R. E.; and Rieppel, P. J.: Methods of Evaluating Welded Joints. DMIC Rept. 165, Battelle Memorial Institute, Defense Metals Information Center, 1961.
7. Nickel Alloy Steel Data Book. Bul. C, sec. 4, International Nickel Co., 1975, p. 25.

TABLE I. - FRACTURE TOUGHNESS PROPERTIES OF GAS-TUNGSTEN

ARC WELDED Fe-12Ni ALLOYS USING 0.7-

CENTIMETER-THICK PLATE

Condition		Weld cooling rate, °C/sec	Fracture toughness, K_{Icd} , MPa \sqrt{m}			
Preweld	Postweld		At -196 ^o C		At 25 ^o C	
			Weld	HAZ ^a	Weld	HAZ ^a
Fe-12Ni-0.25Ti alloy						
Base alloy ^{b,c}	-----	--	275	275	276	276
Hot rolled	None	44	227	286	---	---
Hot rolled	Heat treated ^c	44	258	269	---	---
Heat treated ^c	None	44	231	347	188	264
Heat treated ^c	None	81	262	366	186	280
Heat treated ^c	None	2	196	293	169	279
Fe-12Ni-0.5Al alloy						
Base alloy ^{b,d}	-----	--	284	284	320	320
Hot rolled	None	44	77	71	---	---
Hot rolled	Heat treated ^d	44	275	300	---	---
Heat treated ^d	None	44	69	81	104	169
Heat treated ^d	None	81	85	102	---	311
Heat treated ^d	None	2	77	71	109	194
Fe-12Ni-0.25Nb alloy						
Base alloy ^{b,e}	-----	--	329	329	242	242
Hot rolled	None	44	81	205	---	---
Hot rolled	Heat treated ^e	44	213	320	---	---
Heat treated ^e	None	44	47	67	71	147
Heat treated ^e	None	81	78	180	116	285
Heat treated ^e	None	2	131	81	133	135

^aHeat-affected zone.^bData from ref. 3.^cAnnealed 2 hr at 685° C and water quenched.^dAnnealed 2 hr at 550° C and water quenched.^eAnnealed 2 hr at 820° C and water quenched.

TABLE II. - TENSILE PROPERTIES OF AUTOGENOUS GAS-TUNGSTEN ARC WELDED

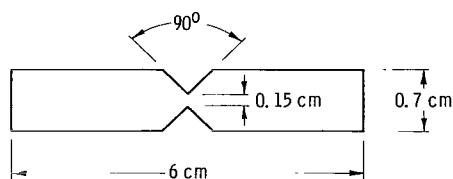
Fe-12Ni ALLOYS USING 0.1-CENTIMETER-THICK SHEET

Condition		Weld cooling rate, °C/sec	-196° C test temperature				25° C test temperature			
Preweld	Postweld		Yield strength, MPa	Ultimate tensile strength, MPa	Elongation, percent	Location of fracture	Yield strength, MPa	Ultimate tensile strength, MPa	Elongation, percent	Location of fracture
Fe-12Ni-0.25Ti alloy										
Base alloy ^a	-----	---	979	1062	19	-----	621	696	9	-----
Hot rolled	None	63	924	986	11	Base alloy	600	655	6	Base alloy
Hot rolled	Heat treated ^b	63	834	917	11	↓	517	600	8	↓
Heat treated ^b	None	63	924	993	11	↓	579	641	9	↓
Heat treated ^b	None	142	917	979	12	↓	579	655	8	↓
Heat treated ^c	None	3	924	979	11	↓	586	641	8	↓
Fe-12Ni-0.5Al alloy										
Base alloy	-----	---	1110	1220	14	-----	752	855	6	-----
Hot rolled	None	63	1020	1069	7	Base alloy	683	717	4	Base alloy
Hot rolled	Heat treated ^d	63	869	917	17	↓	572	607	14	↓
Heat treated ^d	None	63	910	951	12	↓	572	627	10	↓
Heat treated ^d	None	142	883	938	13	↓	552	593	9	↓
Heat treated ^c	None	3	903	965	10	↓	565	614	9	↓
Fe-12Ni-0.25Nb alloy										
Base alloy	-----	---	1055	1145	18	-----	689	786	7	-----
Hot rolled	None	63	1000	1062	11	Base alloy	703	731	6	Base alloy
Hot rolled	Heat treated ^e	63	903	1020	11	Base alloy	593	683	7	Weld
Heat treated ^e	None	63	965	1014	6	Weld	648	703	8	Base alloy
			945	945	Nil	Weld				
Heat treated ^e	None	142	958	1007	11	Base alloy	641	689	6	Base alloy
Heat treated ^c	None	3	979	1027	10	Base alloy	634	676	7	Base alloy
			972	1020	9	Base alloy				
			821	821	Nil	Weld				

^aHot rolled.^bAnnealed 2 hr at 685° C and water quenched.^cPreheated to 260° C for welding.^dAnnealed 2 hr at 550° C and water quenched.^eAnnealed 2 hr at 820° C and water quenched.

TABLE III. - CHEMICAL ANALYSIS OF WELD METAL AND UNAFFECTED
BASE ALLOY OF FOUR-PASS GAS-TUNGSTEN ARC WELD JOINTS

	Analyzed alloy content, at. %				Analyzed interstitial content, ppm by weight		
	Ni	Al	Nb	Ti	O	N	C
Fe-12Ni-0.25Ti:							
Weld	-----	-----	-----	0.21	14	13	144
	-----	-----	-----	-----	70	16	---
Base alloy	-----	-----	-----	.26	16	12	160
	-----	-----	-----	-----	20	13	---
Fe-12Ni-0.5Al:							
Weld	11.94	0.41	-----	-----	38	8	145
Base alloy	12.00	.45	-----	-----	29	6	187
Fe-12Ni-0.25Nb:							
Weld	-----	-----	0.21	-----	92	24	56
Base alloy	-----	-----	.22	-----	14	20	132
Transfer efficiency across arc, percent	99	91	95	81	--	--	---



(a) WORKPIECE PREPARATION BEFORE WELDING.



(b) SUBSEQUENT AS-WELDED CONFIGURATION
SHOWING WELD-PASS SEQUENCE.

Figure 1. - Gas-tungsten arc (GTA) weld joint.

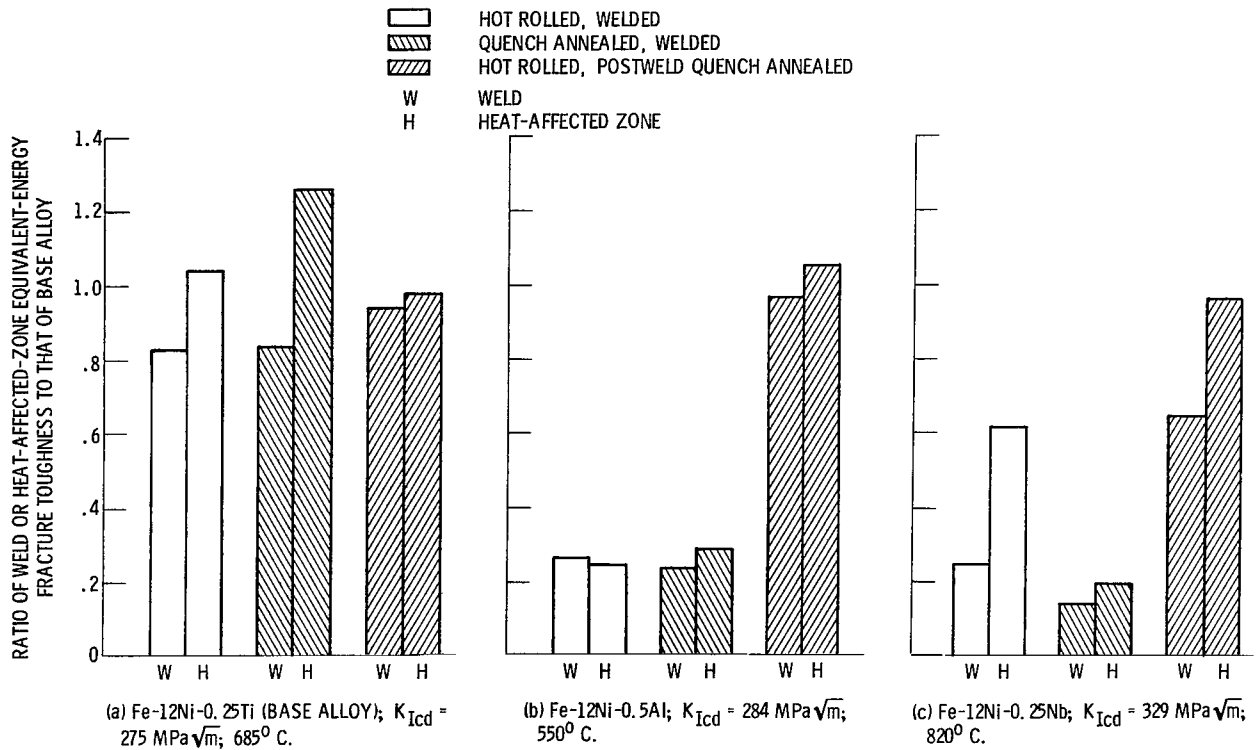


Figure 2. - Effects of pre- and postweld heat treatments on -196°C fracture toughness of welded Fe-12Ni alloys compared with that of the base alloy heat treated for maximum toughness, for various values of equivalent-energy fracture toughness K_{Icd} and annealing temperatures.

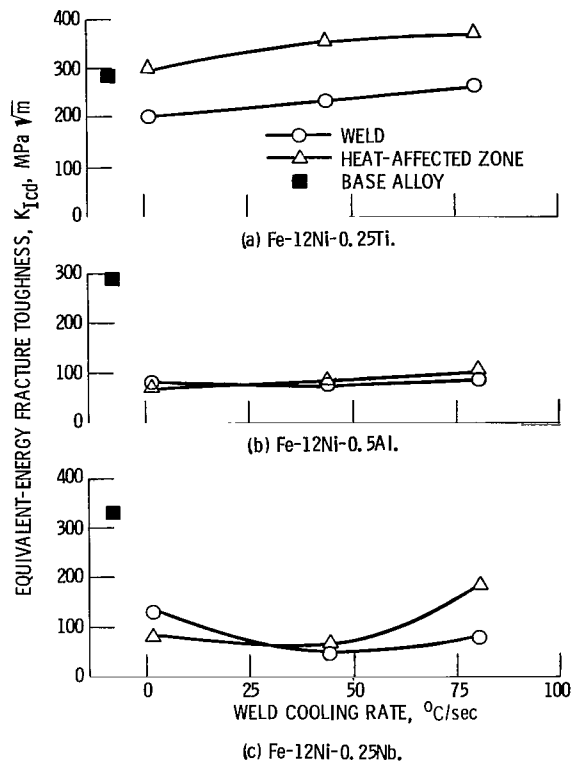


Figure 3. - Effect of weld cooling rate on the $-196^{\circ}C$ fracture toughness of Fe-12Ni alloys. (Reference base alloy was heat treated for maximum toughness.)

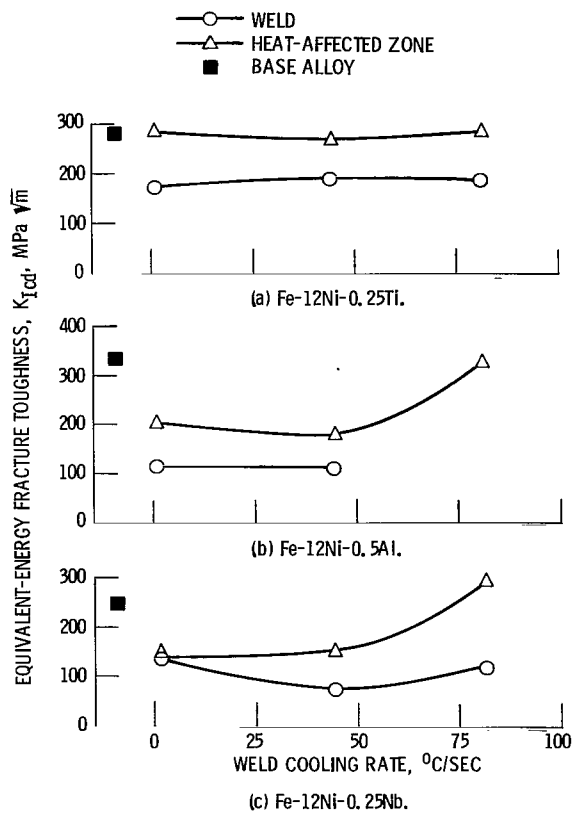


Figure 4. - Effect of weld cooling rate on $25^{\circ}C$ fracture toughness of Fe-12Ni alloys. (Reference base alloy was heat treated for maximum toughness.)

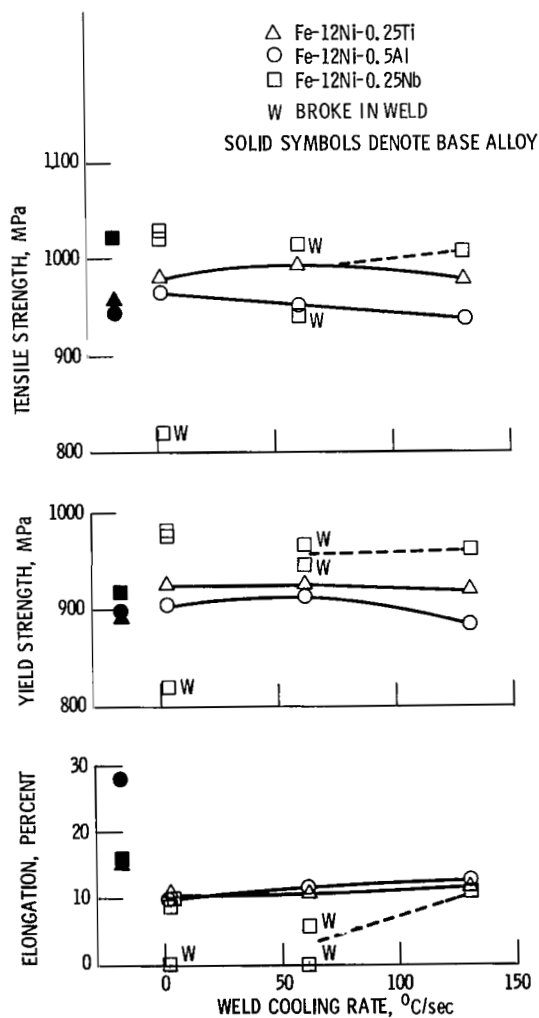


Figure 5. - Effect of weld cooling rate on transverse-weld tensile properties of Fe-12Ni alloys tested at -196°C . (Properties of base alloy, heat treated for maximum toughness, are shown for comparison (ref. 3).)

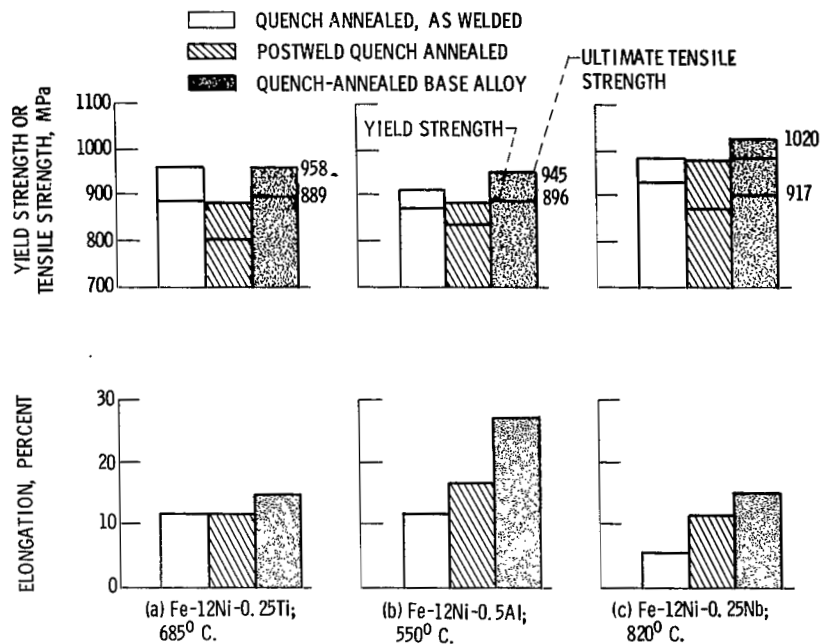


Figure 6. - Transverse-weld tensile properties of gas-tungsten arc welded 0.1-centimeter-thick Fe-12Ni alloys tested at -196°C , and annealed at various temperatures.

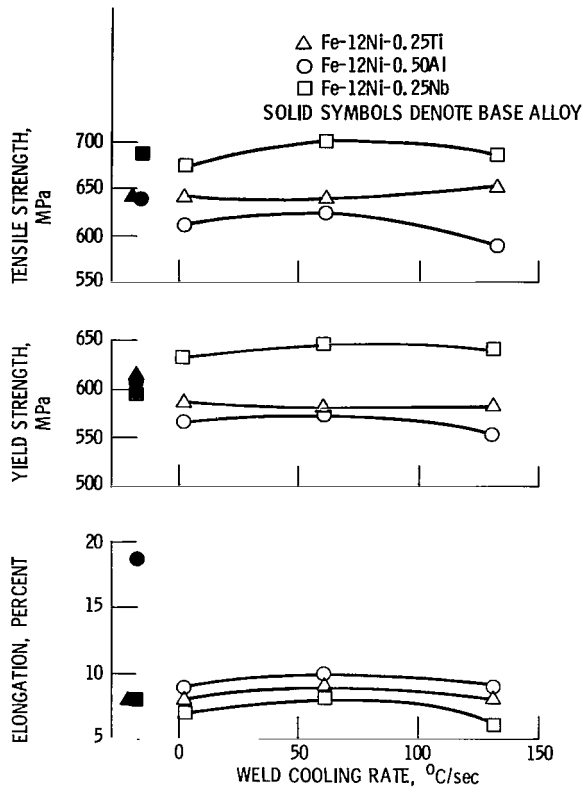
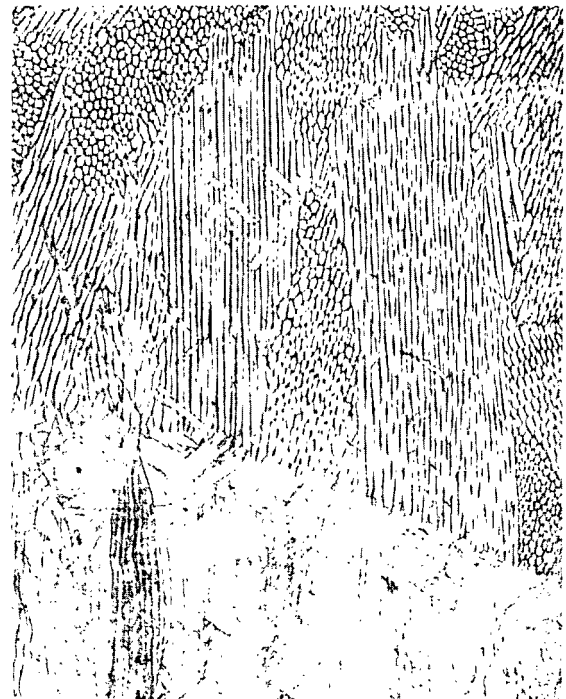


Figure 7. - Effect of weld cooling rate on transverse-weld tensile properties of Fe-12Ni alloys tested at 25° C. (Properties of base alloy, heat treated to maximum toughness, are shown for comparison (ref. 3).)



(a) As welded.



(b) Postweld quench annealed at 550° C.

Figure 8. - Typical cellular solidification structure of Fe-12Ni-0.5Al weld metal. Etchant, Nital; X100.

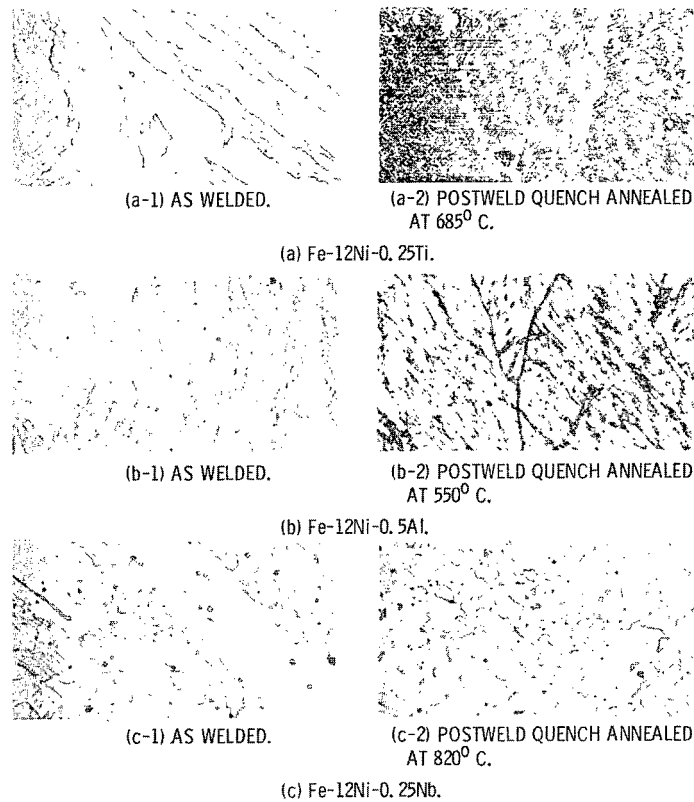


Figure 9. - Weld microstructures of Fe-12Ni alloys as welded and postweld quench annealed at 685°, 550°, and 820° C. Etchant, three acids; X750.

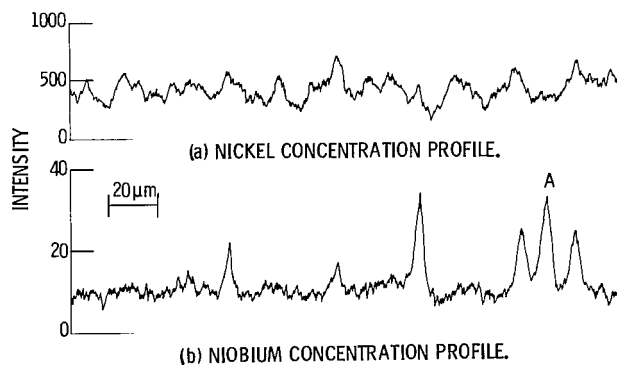


Figure 10. - Segment of electron microprobe line scan for nickel and niobium in gas-tungsten arc welded Fe-12Ni-0.25Nb.



110 001 C1 U C 770204 S00903DS
DEPT OF THE AIR FORCE
AF WEAPONS LABORATORY
ATTN: TECHNICAL LIBRARY (SUL)
KIRTLAND AFB NM 87117

POSTMASTER: If Undeliverable (Section 158
Postal Manual) Do Not Return

"The aeronautical and space activities of the United States shall be conducted so as to contribute . . . to the expansion of human knowledge of phenomena in the atmosphere and space. The Administration shall provide for the widest practicable and appropriate dissemination of information concerning its activities and the results thereof."

—NATIONAL AERONAUTICS AND SPACE ACT OF 1958

NASA SCIENTIFIC AND TECHNICAL PUBLICATIONS

TECHNICAL REPORTS: Scientific and technical information considered important, complete, and a lasting contribution to existing knowledge.

TECHNICAL NOTES: Information less broad in scope but nevertheless of importance as a contribution to existing knowledge.

TECHNICAL MEMORANDUMS: Information receiving limited distribution because of preliminary data, security classification, or other reasons. Also includes conference proceedings with either limited or unlimited distribution.

CONTRACTOR REPORTS: Scientific and technical information generated under a NASA contract or grant and considered an important contribution to existing knowledge.

TECHNICAL TRANSLATIONS: Information published in a foreign language considered to merit NASA distribution in English.

SPECIAL PUBLICATIONS: Information derived from or of value to NASA activities. Publications include final reports of major projects, monographs, data compilations, handbooks, sourcebooks, and special bibliographies.

TECHNOLOGY UTILIZATION PUBLICATIONS: Information on technology used by NASA that may be of particular interest in commercial and other non-aerospace applications. Publications include Tech Briefs, Technology Utilization Reports and Technology Surveys.

Details on the availability of these publications may be obtained from:

SCIENTIFIC AND TECHNICAL INFORMATION OFFICE

NATIONAL AERONAUTICS AND SPACE ADMINISTRATION
Washington, D.C. 20546